Grid Controllability Aware Optimal Placement of PMUs with Limited Input Current Channels

Akash Kumar Mandal, Swades De, and Bijaya Ketan Panigrahi
Department of Electrical Engineering and Bharti School of Telecommunication and Management
Indian Institute of Technology Delhi, New Delhi 110016, India.

***Abstract*—This paper proposes a novel approach for optimal placement of phasor measurement units (PMUs) targeting smart grid controllability under perturbed system conditions while ensuring system observability. In determining the optimal number of required PMUs, as a practical consideration, PMUs are considered to have limited number of input channels. A weighted least square optimization problem with a continuous relaxation is considered for the discrete binary constraint. A perturbation-robust algorithm is developed for a global optimal solution that achieves optimal PMU placement. The efficacy of the proposed smart grid monitoring instrumentation approach is validated on IEEE 6, 14, 30, 57, and 118-bus systems. The grid perturbations are represented with node weights using a small signal modeling approach. The results demonstrate that, unlike the conventional system observability-aware PMU deployment, the proposed instrumentation strategy ensures system controllability under generic perturbation conditions with a revised PMU placement vector of reduced size in all the test cases.**

***Index Terms*—Grid controllability, grid monitoring instrumentation, limited input current channels, optimal PMU placement, perturbation, phasor measurement unit (PMU)**

I. Introduction

Proliferation of power electronic switching based loads and renewable energy sources into the conventional power grid has led to manifold increase of sustained as well as sporadic perturbations in the recent years [1]. Prevalence of such perturbed system states motivates the need for a revised instrumentation for real-time monitoring and estimation in the modern power networks [2]. The advanced instrumentation of the power grid includes the integration of phasor measurement units (PMUs), which communicate the real-time measurements of critical grid attributes to a phasor data concentrator (PDC), for the purpose of monitoring and control [3]. System state estimation at the PDC is compounded by the errors due to electromagnetic noise from power lines during PMU data transmission [4]. Therefore, beyond ensuring observability under normal operating conditions, PMU deployment strategy also needs to guarantee accurate system state estimation at the PDC under perturbed grid conditions. In this work, controllability is defined as the ability of the optimally deployed PMUs with limited input current channels to estimate a perturbed grid health at the PDC within acceptable error bounds.

A. Literature Review and Motivation

The related work on smart grid monitoring instrumentation can be broadly divided into three sets. The first set [5], [6] presents various strategies for optimal PMU placement at minimized deployment cost while maintaining a basic grid observability. They do not consider the notion of grid controllability owing to proper system state reconstruction at the PDC under perturbed system conditions. This limits the applicability of such approaches in modern grids where renewable penetration causes sustained oscillations. These studies also do not consider the practical constraint of limited input current channels of the PMUs. Therefore, optimized PMU deployment solutions rendered by these existing approaches need to be revisited to address the practical scenarios.

The second set of work employ different statistical approaches [7], [8], and evolutionary algorithms [9], [10], for optimal PMU placement in various grid topologies. They aim at devising unique optimal placement solutions within a given time constraint. Though time complexity reduction in optimal PMU placement is an important objective, the key practical aspects, namely, realistic PMU capabilities, accounting for grid perturbation, and grid controlability beyond only observability, require further research attention.

The final set [11], [12] look into the optimal PMU placement considering different system adversities. These works analyze the PMU placement variations under different line and PMU outages. The studies in [13] and [14] analyze a multi-stage PMU installation process for co-phasing while ensuring complete system observability. The work in [15] further analyzed the use of the installed PMUs in outage detection in power networks. However, with the notion of micro-grid, perturbed grid states are more predominant over grid faults now-a-days. Thus, a continuum between ideal and faulty grid states are of current interest, which call for revisiting the optimal PMU placement strategy.

As highlighted above, optimal PMU placement under grid perturbation is an important aspect that requires research attention. Additionally, to the best of our knowledge, the impact of limited input current channels in practical PMUs on the estimation accuracy of real power networks under perturbation remains unexplored in the literature. To this end, this paper proposes perturbation-immune optimal placement of PMUs with limited input current channels, from a redefined notion of grid controllability.

B. Contributions and Significance

In view of the lacuna in the literature on instrumentation of smart grid for monitoring and controllability under perturbations, we revisit the optimum PMU deployment strategy. The key contributions of this work are as follows:

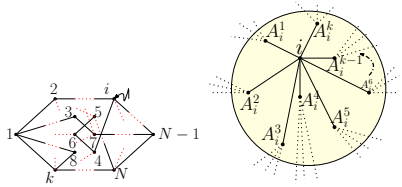

(a) (b)

Fig. 1: (a) N-node smart grid network graph, (b) incidence diagram for node i with k incident lines.

1) The notion of line observability reward and node weight vector is proposed for efficient grid health characterization under random perturbations.
2) A minimum-cost non-linear weighted least square (WLS) minimization problem is formulated ensuring grid controllability under perturbations.
3) A novel polynomial grid observability constraint is proposed while considering the presence or absence of zero injection bus (ZIB), followed by the modeling of line observability reward and node weights.
4) The two-stage optimization problem formulation is validated for IEEE 6, 14, 30, 57, and 118-bus systems, establishing the importance of the proposed perturbation-robust PMU placement strategy.

Simulation results demonstrate that the proposed grid controllability-aware PMU deployment is able to capture the grid health under perturbations, which is otherwise not possible in the conventional deployment strategy.

II. System Model for Optimal PMU Placement

Consider a power grid with a set of buses indexed by $\mathscr{N} := \{1, 2, \cdots, N\}$. The buses are connected through a set of transmission lines $\mathscr{L} \subset \mathscr{N} \times \mathscr{N}$, i.e. , bus i is connected to bus j iff $(i, j) \in \mathscr{L}$. Accordingly, $\mathbf{A}_i$ is the set of buses incident to bus i, with the element j represented as A_i^j, such that $\|A_i\| = k_i$ is its incidence order as shown in Fig. 1(b). Further, let us define the grid incidence matrix $\mathbf{A} = [a_{i,j}|i, j \in \mathscr{N}]$, such that $a_{i,j} = 1$, iff nodes i and j are connected, and 0 otherwise. Controllability in this work implies the ability to reconstruct the system image at the PDC for monitoring under perturbed system conditions. We consider voltage and current phasor perturbations while formulating the perturbation-robust optimal PMU placement strategy. Perturbations amounting to Δv_i, $\Delta\phi_i$, $\Delta i_{i,j}$, and $\Delta\delta_{i,j}$ against the i-th node's steady state voltage magnitude v_i, voltage phase ϕ_i, current magnitude $i_{i,j}$, and current phase $\delta_{i,j}$ is considered in the mentioned order, as shown in Fig. 1(a), and propagation through all incident lines to node i is considered. All PMUs are considered to have a limited number of input current channels, typically 1, that is less than the minimum node order of the grid. A 50 Hz grid is considered, where the voltage and current readings are recorded at 19200 sps and reported at 200 fps.

III. Optimal PMU Placement Analysis

This section outlines the prerequisites for the controllability-aware optimal PMU placement problem, followed by the optimization problem formulation.

A. Line Observability Reward Formulation

Let us define a variable z_i s.t, $z_i = 1$ or 0 implies the presence or absence of PMU at the i-th bus respectively. Let R out of N grid nodes have a PMU, with the PMU installed at the i-th node having l_i input channels with node order k_i, s.t. $l_i < k_i$. If $\Pr(\mathrm{L}_{i,j})$ signifies the probability that link i-j gets monitored, then we have $\Pr(\mathrm{L}_{i,j}) \triangleq \mathrm{I}\left(\mathrm{L}_{i,j} = 1\right)(z_i x_i + z_j x_j)$, where $\mathrm{I}(\mathrm{L}_{i,j} = 1)$ is a binary indicator function that takes 1 iff node i and j are connected and x_i denotes the random variable representing the probability of link i-j getting monitored by the PMU installed at node i. The randomness results from random selection of lines to be monitored using a PMU with limited input channels, as there is no defined norm for such a selection. Therefore, the average reward for observing the link i-j is given as $\mu_{i,j} = c_{i,j}\mathbb{E}[\Pr(L_{i,j})] = c_{i,j}\mathbb{E}[\mathrm{I}(L_{i,j} = 1)(z_i x_i + z_j x_j)]$, where $c_{i,j}$ is the reward for observing link i-j, and relates to the importance of that node. Further, the order of installation also plays a role in defining this probability. Considering all such orders, the average line observability reward is $\mu_{i,j} = c_{i,j}\mathrm{I}(L_{i,j} = 1)(z_i\mathbb{E}[x_i] + z_j\mathbb{E}[x_j]) = c_{i,j}\mathrm{I}(L_{i,j} = 1)(z_i S_i + z_j S_j)$, where $S_i = \mathbb{E}[x_i] = \sum_{x_i=1}^{l_i} x_i \frac{1}{k_i - (l_i - x_i)} = \frac{1}{k_i - l_i + 1} + \frac{2}{k_i - l_i + 2} + \cdots + \frac{l_i}{k_i}$. On simplifying, we get

$$\begin{aligned} S_i &= \frac{l_i}{k_i} + \frac{l_i - 1}{k_i - 1} + \cdots + \frac{1}{k_i - l_i + 1} = 1 - \sum_{j=1}^{l_i - 1} \frac{(k_i - l_i)}{k_i - j} \\ &\approx 1 - \int_0^{\frac{l_i - 1}{k_i}} \frac{(k_i - l_i)}{1 - x} dx = 1 - (k_i - l_i)\ln\left(1 - \frac{l_i - 1}{k_i}\right). \end{aligned} \tag{1}$$

S_i denotes the average number of input current channels monitoring the link i-j using a PMU installed at node i. Thus, the average line observability reward matrix is given as

$$\mathbf{A}_l = \begin{bmatrix} \mu_{1,1} & \mu_{1,2} & \cdots & \mu_{1,N} \\ \vdots & \vdots & \ddots & \vdots \\ \mu_{N,1} & \mu_{N,2} & \cdots & \mu_{N,N} \end{bmatrix} = \mathbf{c} \odot \mathbf{A} \odot \mathbf{d} \tag{2}$$

where $\odot$ denotes a Hadamard product, $\mathbf{A}$ is the grid incidence matrix, $\mathbf{c}$ is the reward matrix with the (i,j) entry defined as $c_{i,j}$, and $\mathbf{d} = \mathbf{v}^T\mathbb{1} + \mathbf{I}\mathbf{v}$ such that $\mathbb{1} = [1, 1, \cdots, 1]_N^T$, $\mathbf{I} = \mathrm{diag}\left(\mathbb{1}_1, \mathbb{1}_2, \cdots, \mathbb{1}_N\right)$ is a matrix of dimension $N \times N$ with its i-th diagonal entry $\mathbb{1}_i$ being a vector of ones having a zero only at i-th position. Using the above formulations in (2), we get $A_l = c \odot A \odot \left(\mathbf{v}^T\mathbb{1} + \mathbf{I}\mathbf{v}\right)$. Further, $\mathbf{v} = \mathbf{S}\mathbf{z}$ is defined for the sake of concise representation, such that $\mathbf{S}$ is diagonal, and the (i, i) entry in $\mathbf{S}$ is defined as S_i, as in (1). Let the node weight vector be defined as $\boldsymbol{\omega}$ with ω_i the weight for the i-th node. Then, the aggregate grid observability index (AGOI) is defined as $\boldsymbol{\omega}^T c \odot A \odot \left(\mathbf{z}^T\mathbf{S}^T\mathbb{1} + \mathbf{I}\mathbf{S}\mathbf{z}\right)\boldsymbol{\omega}$.

Further, the importance of observing the link i-j stems from the Thevenin equivalent impedance between the nodes. The Thevenin equivalent impedance between node i-j $\forall i, j \in \mathscr{N}$ given by $\mathbb{Z}_{i,j}$ is calculated using the Z bus matrix algorithm. It gives a sense into the ability of a node pair to destabilize the network under perturbation. In the scope of this work, we define $c_{i,j} = \frac{\mathbb{Z}_{i,j}}{\sum_{i=1}^{N} \mathbb{Z}_{i,j}}$, as the reward for observing link i-j. Further, controllability for the i-th node is defined as $o_i = \sum_{j \in \mathbf{A}_i} \mu_{i,j}$, with the controllability vector defined by

$\mathbf{O}^T$. The definition of node weight vector by considering perturbations in the voltage magnitude of the concerned node is proposed in Lemma 1.

Lemma 1. *The weight of the j-th node is defined as*

$$\omega_j = (\sin(\omega t + \phi_j) \sum_{r=1}^{k_j} z_{j_r,j}^{-1})(\sum_{r=1}^{k_j} \sin(\omega t + \phi_{j_r}) z_{j_r,j}^{-1} \alpha_{j_r})^{-1}$$

where $\Delta v_{j_r} = \alpha_{j_r} \Delta v_0$, where Δv_0 is the instability grid node voltage change and α_{j_r} is a constant of multiplication, $\omega = 2\pi f$ is the angular grid frequency, t represents time, $z_{i,j} = \sqrt{r_{i,j}^2 + x_{i,j}^2}$ is the impedance of link i-j, with $r_{i,j}$, and $x_{i,j}$ denoting the link resistance and reactance, respectively.

Proof. See Appendix A. □

B. Formulation of Optimal PMU Placement Problem

A non-linear WLS minimization problem is formulated in $\mathbf{F}_1$ which aims at making the grid observable with minimum number of PMUs, and optimum network controllability, based on maximizing the grid controllability under perturbation, is ensured by maximizing $\mathbf{F}_2$ in (3) as follows

$$\begin{aligned} &\mathbf{F}_1 : \text{Min } \{\mathbf{z}^T \mathbf{C}_{\text{P}} \mathbf{z} + \mathbf{G}(\mathbf{z})^T \mathbf{V} \mathbf{G}(\mathbf{z})\} \\ &\mathbf{F}_2 : \text{Max } \mathbf{O}^T \mathbf{c} \mathbf{O} \text{ s.t. } \mathbf{C}_1 : \mathbf{z} \in \mathscr{D}_R \end{aligned} \tag{3}$$

where $\mathbf{C}_1$ defines the possibility space of the variable $\mathbf{z}$ representing the presence of PMU at N nodes, s.t. $\mathscr{D}_R := \left\{ \mathbf{z} \in \{0,1\}^N \,\middle|\, \sum_{i \in \mathscr{N}} z_i = R \right\}$, $\mathbf{C}_{\text{P}} = c\mathbf{I}_{\text{N}}$, with c denoting the per PMU cost, $\mathbf{G}(\mathbf{z}) = [g_1(\mathbf{z}), \cdots, g_2(\mathbf{z})]^T$, $\mathbf{V} = \mathbf{v}^T \odot \mathbf{I}_{\text{N}}$, with $\mathbf{v} = [v_1, \cdots, v_{\text{N}}]^T$ denoting the unobservability cost for the nodes $i \in \{1, \cdots, \text{N}\}$, $\mathbf{O} = [o_1, o_2, \cdots, o_N]$, with $o_i = \sum_{j \in \mathbf{A}_i} \mu_{i,j}$, and $\mathbf{c} = [c_{i,j}]_{i,j \in \{1,\cdots,N\}}$, with $c_{i,j} = \frac{\mathbb{Z}_{i,j}}{\sum_{i=1}^{N} \mathbb{Z}_{i,j}}$, where $\mathbb{Z}_{i,j}$ denotes the Thevenin equivalent impedance of link i-j. This cost is set high to ensure a binary (0 or 1) PMU assignment to the respective buses. In this work we define a polynomial observability function $g_i(\mathbf{z}) \in \{g_{i,\overline{ZIB}}(\mathbf{z}), g_{i,ZIB}(\mathbf{z})\}$ for node i, with the two functions capturing the aspect of not considering or considering the impact of ZIB respectively. Neglecting ZIB we have

$$g_{i,\overline{ZIB}}(\mathbf{z}) = \sigma_i - z_i - \sum_{j \in A_i} z_j, \, \forall i \in \{1, \cdots, N\} \tag{4}$$

where σ_i is the redundancy order for the i-th node, denoting total PMUs monitoring that node, and $\mathbf{A}_i$ is the set containing nodes incident to node i. A joint weighted optimization problem from (3) can be formulated as

$$(\mathbf{P}_1) : \text{Min J}(\mathbf{z}) = \mathbf{F}_1 - \lambda \mathbf{F}_2 \text{ s.t. } \mathbf{C}_1 \tag{5}$$

where $\lambda \in \{0, 1\}$ is a binary weight, outlining the choice seeking either a controllability-aware optimal PMU placement solution with $\lambda = 1$, or conventional optimality with $\lambda = 0$. It is notable that the controllability-aware optimization perspective dwells on optimum grid observability and control under perturbed grid conditions using limited number of practical PMUs with one input channel. Furthermore, ZIBs are the nodes that cause no current injection into the system. Thus, if all buses incident to a ZIB are observable except one, the unobserved bus can be made observable by applying KCL at the ZIB. Further, if all buses incident to the ZIB are observable except the ZIB, it can be made observable by applying KCL at the ZIB. Let t_i be a binary parameter taking 1 iff bus i is a ZIB, and $y_{i,j}$ be an auxiliary binary variable corresponding to bus i and j, such that $j \in \mathbf{A}_i$. If $Y_i = \{y_{i,j}\}$, then $\|Y_i\| = \|\mathbf{A}_i\| + t_i$. Therefore, the observability constraint defined in (4) modifies to (6) under the considerations of ZIB

$$g_{i,ZIB}(\mathbf{z}) = \sigma_i - z_i - t_i y_{i,i} - \sum_{j \in A_i} (z_j + t_j y_{i,j}) \tag{6}$$

with all notations as defined previously. Thus, the proposed PMU placement problem including ZIB can be given by updating $g_i(\mathbf{z})$ in (3) and substituting in (5). The next lemma provides a continuous relaxation for the constraint $\mathbf{C}_1$.

Algorithm 1: Penalty-aware Perturbation Robust Optimal PMU Placement Algorithm

1 : **Initialization**: Set $\kappa = 0$. Choose a feasible point $\mathbf{z}^{(0)} \in (0,1)^N$ using Algo. 2
2 : Find δ s.t. $f(\mathbf{z}^{(0)})$ and $\frac{1}{R} - \frac{1}{\phi(\mathbf{z}^{(0)})}$ get equal significance.
3 : Set $\kappa \to \kappa + 1$.
4 : Solve (9) using Algo. 2 for the next feasible point $\mathbf{z}^{(\kappa+1)}$.
5 : **Until** convergence.

Lemma 2. *For a polytope Poly($\mathscr{D}_R$), the discrete constraint $\mathbf{C}_1$ is equivalent to the continuous constraint $\mathbf{z} \in$ Poly $(\mathscr{D}_R)$, $\phi(\mathbf{z}) \geq R$ for $\phi(\mathbf{z}) := \sum_{i \in \mathscr{N}} z_i^{\beta}$ with $\beta > 1$.*

Proof. See Appendix B. □

Since, $\phi(\mathbf{z})$ is convex in $\mathbf{z}$, the constraint $\phi(\mathbf{z}) \geq R$ is a reverse convex constraint. As such, it is a difference of two convex sets, Poly($\mathscr{D}_R$) and $\{\mathbf{z} | \phi(\mathbf{z}) < R\}$. Also, as β decreases, $\phi(\mathbf{z})$ tends to a linear function. However, as $\beta \to 1$, the function $\phi(\mathbf{z}) - R$ approaches zero very quickly.

Proposition 1. *$\tilde{\phi}(\mathbf{z}) = \frac{1}{\phi(\mathbf{z})} - \frac{1}{R}$ can be used to measure the degree of satisfaction of the discrete constraint $\mathbf{C}_1$ in the sense that $\tilde{\phi}(\mathbf{z}) \geq 0 \; \forall \mathbf{z} \in$ Poly($\mathscr{D}_R$) and $\tilde{\phi}(\mathbf{z}) = 0$ iff $\mathbf{z} \in \mathscr{D}_R$.*

C. Solution to Optimal PMU Placement Problem

This subsection details the analysis of the optimal solution to ($\mathbf{P}_2$). Using Lemma 2 and Proposition 1 in ($\mathbf{P}_2$), we formulate a penalized optimization problem as

$$\min_{\mathbf{z}} F_\delta(\mathbf{z}) := \mathbf{J}(\mathbf{z}) + \delta \tilde{\phi}(\mathbf{z}) \text{ s.t. } \mathbf{z} \in \text{Poly}(\mathscr{D}_R) \tag{7}$$

where $\delta > 0$ is a penalty parameter. This penalized optimization problem is exact with a sufficiently large δ. It is notable that (7) is a minimization of a non-convex function over a convex set. However, by achieving the minimum for $F_\delta(\mathbf{z})$, an efficient PMU deployment strategy can be obtained under perturbed grid conditions with ambient grid estimation at the PDC. The pseudo-code for the proposed computational procedure used in finding the optimal solution to ($\mathbf{P}_2$) is given

Algorithm 2: Feasible Point Generation Algorithm

1 : Fetch generation counter $t = \kappa$
2 : **If** $t = 0$, create initial population of P vectors $\mathbf{P}^0 = \{\mathbf{z}_1^0, \mathbf{z}_2^0, \cdots, \mathbf{z}_P^0\} \subset \mathscr{D}_R$, s.t. $\|\mathbf{P}^t\| = P\ \forall t$
Otherwise, Use $\mathbf{P}^{t+1}$ generated in previous iteration
3 : Compute fitness value α_i^t of each vector in $\mathbf{P}^t$
4 : Choose $\mathbf{z}^{(\kappa)} \rightarrow \mathbf{z}_i^t$ having maximum α_i^t and set $t \rightarrow t+1$
5 : $p_0^t :=$ no. of vectors in $\mathbf{P}^t$ with $\alpha_i \geq \eta\alpha_{\max}$
6 : $\mathbf{V}_P^t :=$ set of those p_0^t vectors from $\mathbf{P}^t$
7 : Set $p_1^t = 2$, $p_2^t = 1$; generate crossover and mutation vectors using steps 8-9
8 : **Crossover vectors**: $\mathbf{V}_{CO}^t = C\left(\mathbf{V}_P^t, p_1^t\right)$
9 : **Mutation vectors**: $\mathbf{V}_M^t = M\left(\mathbf{V}_P^t, p_2^t\right)$
10 : Calculate fitness for these vectors, increment $p_1^t \rightarrow p_1^t + 1$ and $p_2^t \rightarrow p_2^t + 1$
11 : Repeat steps 8-11 till fitness for all vectors $\geq \eta\alpha_{\max}$
12 : Choose best P vectors from these based on fitness
13 : **Update**: $\mathbf{P}^t \rightarrow \mathbf{P}^{t+1}$ using the selected P vectors.

TABLE I: Optimal hyper-parameter settings and convergence details of Algorithm 1; $\beta = 1.45$, c.t.: convergence time.

Test system	ϵ	δ	c.t. (s) ($\lambda = 1$)	c.t. (s) ($\lambda = 0$)
IEEE 6-bus	0.27	0.09	43.12	43.37
IEEE 14-bus	0.36	0.10	62.94	60.77
IEEE 30-bus	0.57	0.10	79.14	76.53
IEEE 57-bus	1.00	1.00	80.47	80.37
IEEE 118-bus	1.20	1.00	216.31	216.19

in Algorithms 1. However, as $\phi(\mathbf{z})$ is convex, we have

$$\begin{aligned}\phi(\mathbf{z}) \geq & \phi^{(\kappa)}(\mathbf{z}) := \phi(\mathbf{z}^{(\kappa)}) + \langle \nabla\phi(\mathbf{z}^{(\kappa)}), \mathbf{z} - \mathbf{z}^{(\kappa)} \rangle \\ = & -(\beta - 1)\sum_{i \in \mathscr{N}} (\mathbf{z}_i^{(\kappa)})^{\beta} + \beta \sum_{i \in \mathscr{N}} (\mathbf{z}_i^{(\kappa)})^{\beta - 1}\mathbf{z}_i \end{aligned} \tag{8}$$

where $\langle u, v \rangle$ denotes the inner product between the vectors u and v. Therefore, an approximate upper bound for $\frac{1}{\phi(\mathbf{z})}$ at $\mathbf{z}^{(\kappa)}$ can be obtained as $\frac{1}{\phi(\mathbf{z})} \leq \frac{1}{\phi^{(\kappa)}(\mathbf{z})}$ over the trust region $\phi^{(\kappa)}(\mathbf{z}) > 0$. Thus, at the κ-th iteration, following convex optimization needs to be solved to generate $\mathbf{z}^{(\kappa+1)}$

$$\begin{aligned}(\mathbf{P}_3) : \min_{\mathbf{z}} F_{\delta}^{(\kappa)}(\mathbf{z}) :=& \mathbf{J}(\mathbf{z}) + \delta\left(\frac{1}{\phi^{(\kappa)}(\mathbf{z})} - \frac{1}{R}\right) \\ & \text{s.t. } \mathbf{z} \in \text{Poly}(\mathscr{D}_R),\ \phi^{(\kappa)}(\mathbf{z}) > 0. \end{aligned} \tag{9}$$

$(\mathbf{P}_3)$ is solved using Algorithm 2 to generate the next feasible point. We compute the fitness of the i-th vector in $\mathbf{P}^t$ as the normalized value of $f(\mathbf{z})$ in $(\mathbf{P}_2)$, given by $\alpha_i = \frac{f(\mathbf{z}_i^t)}{\sum_{i=1}^{P} f(\mathbf{z}_i^t)}$. Partially matched crossover and simple inversion mutation are used respectively in crossover and mutation operations. In this work, $\eta = 0.9$ is chosen to generate successive feasible points.

IV. Results and Discussion

The proposed optimal PMU placement strategy is compared with the conventional approaches with sufficient input current channels [5], [6], and with limited input current channels [16], [17], [18]. The results are verified for IEEE 6, 14, 30, 57, and 118-bus systems. Algorithm 1 is implemented in E3-1285 v6 CPU; the optimal hyper-parameters are listed in Table I. No direct redundancy was offered to any node, i.e., $\sigma_i = 1$, $\forall i$.

TABLE II: Optimal PMU placement in perturbed IEEE 6-bus system; Conv.: conventional, Rev.: revised, CC: current channels

No. of CC per PMU (rev.)	Conv. opt. PMU placement (suff. CC)	Rev. opt. PMU placement
1	4, 5	1, 3, 5
2	4, 5	3, 6
3	4, 5	4, 5

A. Test Case: Demonstration of Optimal Placement of PMUs with Limited Input Current Channels in IEEE 6-Bus System

For an IEEE 6-bus system, by setting $\lambda = 0$ we get the optimal PMU placement considering grid observability only, as given in Table II. However, when a perturbed system is considered, line observability gains significance over node-based grid observability. From the updated solution using (7), the optimum PMU placement changes, both in number and locations. This proves that the conventional placement strategy is insufficient to monitor actual power grids, considering its perturbations. In contrast, with the notion of controllability-aware PMU placement strategy as proposed in this paper, it is able to provide better line observability with increased grid observability index, as observed from Fig. 2(b).

From Table II we infer that, for a perturbed system the optimal PMU deployment locations and the number of PMUs depend on the number of input current channels in a PMU. Typically the number of input current channels is considered unlimited thus far in literature. In the simulations, it was noted that, for a 6-bus system, optimum controllability is attained when PMUs are installed at bus $\{2, 4, 6\}$ with 1 input current channel per PMU, while the vector updates to $\{3, 6\}$ considering 2 input current channels. However, as the number of input current channels per PMU reach 3, the maximum node incidence order equals the input current channels available per PMU. In such a case, the optimal PMU placement vector reorients to $\{4, 5\}$, which is the same as that rendered by the conventional placement strategy, owing to fulfilling the sufficiency assumption on the input current channels per PMU. These results demonstrate that optimal PMU placement vector changes with limited number of input current channels per PMU, which is the case in practical PMU devices.

B. Variation of Optimal Placement Policy with PMU's Input Current Channel Limitations in Perturbed Power Networks

Table III shows the optimal PMU placement for standard IEEE test systems suggested by the proposed strategy under normal and perturbed grid conditions. It can be seen that, with the proposed perturbation-robust optimal PMU deployment, the location as well as the number of minimum required PMUs change. Further, contrasting the proposed controllability-aware optimal PMU placement solution with the optimal placement of PMUs with 1 input current channel, it can be noted that the proposed strategy is able to achieve optimum grid observability and controllability at a lesser number of PMUs, placed strategically at different nodes.

Table IV shows the change in optimal PMU deployment considering a perturbed grid in the presence of ZIBs. It was observed that the number of PMUs for optimal grid

TABLE III: Controllability-aware optimal PMU placement (OPP) for different IEEE test systems under perturbation without considering ZIB

Test system	Conventional OPP ($\lambda = 0$)		Controllability-aware OPP ($\lambda = 1$) (1 current channel)
	Sufficient current channels [5], [6]	1 current channel [16], [17], [18]	
14-bus	2, 6, 7, 9	1, 3, 4, 6, 9, 11, 12, 14	2, 4, 6, 7, 9, 13
30-bus	1, 7, 8, 10, 11, 12, 18, 23, 26, 30	1, 2, 4, 5, 6, 10, 12, 13, 15, 16, 18, 19, 24, 27, 29	1, 5, 6, 9, 10, 12, 17, 19, 22, 24, 25, 27, 29
57-bus	2, 6, 10, 12, 19, 22, 25, 27, 32, 36, 41, 45, 46, 49, 52, 55, 57	1, 3, 5, 6, 9, 11, 12, 14, 15, 17, 19, 20, 21, 24, 25, 28, 29, 30, 32, 35, 38, 41, 43, 45, 49, 50, 51, 53, 54, 56	1, 2, 4, 6, 9, 12, 15, 19, 20, 22, 24, 26, 29, 30, 31, 32, 35, 36, 41, 45, 46, 50, 51, 53, 54, 56, 57
118-bus	2, 5, 9, 11, 12, 17, 21, 24, 25, 28, 34, 37, 40, 45, 49, 52, 56, 62, 63, 68, 73, 75, 77, 80, 85, 86, 90, 94, 101, 105, 110, 114	1, 3, 6, 8, 10, 11, 12, 15, 17, 19, 20, 21, 23, 27, 28, 29, 32, 34, 35, 40, 41, 43, 45, 46, 49, 50, 51, 52, 54, 56, 60, 62, 65, 66, 70, 72, 75, 76, 77, 78, 80, 83, 85, 86, 87, 89, 90, 92, 94, 96, 100, 101, 105, 106, 108, 110, 111, 112, 114, 117	1, 2, 5, 9, 10, 11, 12, 15, 17, 21, 22, 25, 26, 28, 29, 34, 35, 37, 40, 45, 46, 49, 52, 53, 56, 62, 63, 68, 72, 75, 76, 77, 80, 84, 85, 87, 89, 92, 94, 96, 100, 105, 107, 110, 114

TABLE IV: Controllability-aware OPP for different IEEE test systems under perturbation considering ZIB

Test system	Conventional OPP ($\lambda = 0$)		Controllability-aware OPP ($\lambda = 1$) (1 current channel)
	Sufficient current channels [5], [6]	1 current channel [16], [17], [18]	
14-bus	2, 6, 9	1, 4, 9, 11, 13	2, 4, 6, 9, 13
30-bus	2, 4, 12, 17, 19, 24	1, 3, 5, 9, 11, 12, 17, 19, 23, 24, 29	1, 2, 4, 6, 7, 12, 17, 19, 24
57-bus	1, 6, 9, 19, 29, 30, 32, 38, 51, 54, 56	1, 3, 6, 9, 12, 15, 19, 20, 25, 28, 29, 30, 32, 35, 38, 41, 49, 50, 51, 53, 54, 56	1, 3, 5, 9, 12, 15, 19, 20, 25, 29, 31, 32, 42, 49, 50, 51, 53, 54, 56
118-bus	2, 11, 12, 17, 21, 23, 28, 34, 40, 45, 49, 52, 56, 62, 71, 75, 77, 80, 85, 87, 90, 94, 102, 105, 110, 115	1, 3, 6, 11, 12, 15, 17, 19, 21, 22, 24, 26, 27, 29, 31, 32, 34, 36, 40, 42, 43, 45, 46, 49, 50, 51, 52, 54, 56, 59, 62, 66, 70, 75, 76, 77, 79, 80, 83, 85, 86, 89, 90, 92, 94, 96, 100, 101, 105, 107, 109, 110, 114	1, 2, 6, 11, 12, 17, 21, 23, 27, 28, 32, 34, 36, 40, 42, 45, 46, 49, 53, 56, 62, 71, 75, 76, 77, 79, 80, 84, 85, 87, 89, 90, 92, 94, 96, 100, 102, 105, 107, 109, 110, 115

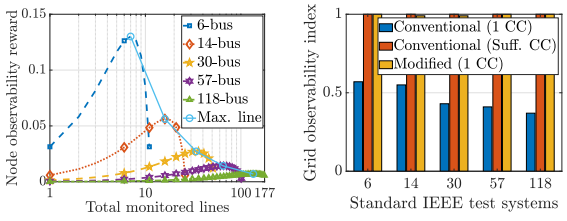

(a) (b)

Fig. 2: (a) Normalized node observability versus total monitored lines, (b) aggregate grid observability for different IEEE test systems.

monitoring drop in this case. However, the optimal deployment vector still differs from the conventional placement scenario. Again, comparing the proposed PMU placement with the conventional deployment of single channel PMUs, it can be inferred that the proposed PMU deployment vector provides superior deployment strategy with reduced number of PMUs and robust grid monitoring under perturbations. For example, in an IEEE 57 and 118-bus network, the number of PMUs, with realistic input current channel capability, required to ensure controllability of a perturbed network reduces by 13% and 20%, respectively. This reduction becomes further prominent as the network dimension increases. Next subsections establish this fact in further details using MMSE, mutual information, and contingency analysis for various deployment scenarios.

C. Variation of Grid Observability

Fig. 2(a) shows the variation of normalized node observability reward defined as $\xi_i = \frac{\sum_{j\in\mathbf{A}_i}\mu_{i,j}}{\sum_{i=1}^{N}\sum_{j\in\mathbf{A}_i}\mu_{i,j}}$ for various IEEE standard test systems, with the total lines monitored in the grid. It provides a very important observation with the number of lines being monitored by the PMUs. It has been considered thus far in literature that all PMUs have sufficient current cards to monitor all incident lines to the nodes on which they are installed. However, with the increase in grid size, such an assumption is not practical. It can be seen from Fig. 2(a) that an optimum normalized node observability reward can be attained with a limited number of direct monitored lines, which translates to limited current cards per PMU. As we try to monitor more than optimal number of lines, the cost of installation increases, leading to a decrease in the reward against observing a node. Thus, a revised placement vector with limited current channels is proposed in Section IV-B.

Fig. 2(b) shows the aggregate grid observability index $\boldsymbol{\omega}^T c \odot A \odot \left(\mathbf{z}^T\mathbf{S}^T\mathbb{1} + \mathbf{I}\mathbf{S}\mathbf{z}\right)\boldsymbol{\omega}$ for different IEEE standard test systems, and contrasts the different optimal PMU deployment scenario. It can be observed that, for conventional PMU deployment, as achieved with $\lambda = 0$ in this work, a normalized aggregate grid observability index of unity is achieved for all grid sizes. It can also be observed that as the assumption is relaxed to achieve the practical device constraint, we observe a significant drop in the grid observability index. This, results in an inefficient grid estimation at the PDC under perturbed system state, as detailed in the next subsection. However, it can be noted that, for the proposed controllability-aware optimal PMU deployment, a normalized grid observability index tending to unity is achieved for all standard grid topologies.

V. Concluding Remarks

This paper proposed a novel power grid monitoring instrumentation strategy for grid controllability under perturbed

conditions, wherein for optimal PMU deployment estimation practical constraint of limited number of input current channels was considered. Line observability reward, node weight vector, and polynomial observability constraint were separately defined that capture a generic grid situation, wherein the grid controllability feature in the optimization was presented through a binary multiplier. The proposed grid monitoring instrumentation strategy gives a handle to define system node weights based on their degree of instability. Simulation of perturbation in different IEEE bus systems of varied size demonstrated that the proposed strategy satisfies the notion of grid controllability with a revised optimal PMU placement vector with a reduction in their number for PMUs with 1 current channel. It was also demonstrated that optimal PMU placement based on observability constraint alone is not sufficient to capture grid health under perturbation.

APPENDIX

A. Proof of Lemma 1

Applying energy balance on link j-j_r, where $j \in A_i$, $r \in [1, \cdots, k_j]$, we have

$$\begin{aligned} v_j \sin(\omega t + \phi_j) =& v_{j_r} \sin(\omega t + \phi_{j_r}) \\ & - i_{j_r,j} z_{j_r,j} \sin\left(\omega t + \delta_{j_r,j} + \theta_{j_r,j}\right) \end{aligned} \tag{A1}$$

where $\omega = 2\pi f$ is the grid frequency, $z_{i,j} = \sqrt{r_{i,j}^2 + x_{i,j}^2}$ is the impedance of link i-j, $\delta_{i,j}$ is the load angle, and $\theta_{i,j} = \tan^{-1}\left(\frac{x_{i,j}}{r_{i,j}}\right)$ with $r_{i,j}$, and $x_{i,j}$ denoting the link resistance and reactance, respectively. Dividing (A1) by $z_{j_r,j}$ and adding it for all incident nodes we have

$$\begin{aligned} \sum_{r=1}^{k_j} \frac{v_j \sin(\omega t + \phi_j)}{z_{j_r,j}} =& \sum_{r=1}^{k_j} \frac{v_{j_r} \sin(\omega t + \phi_{j_r})}{z_{j_r,j}} \\ & - \sum_{r=1}^{k_j} i_{j_r,j} \sin\left(\omega t + \delta_{j_1,j} + \theta_{j_1,j}\right). \end{aligned} \tag{A2}$$

Applying Kirchoff's current law (KCL) at node j in (A2) we have $\sum_{r=1}^{k_j} \frac{v_j \sin(\omega t+\phi_j)}{z_{j_r,j}} = \sum_{r=1}^{k_j} \frac{v_{j_r} \sin(\omega t+\phi_{j_r})}{z_{j_r,j}}$. Introducing small perturbations and linearizing, we get

$$\mathbf{D}_j^T \begin{bmatrix} \Delta v_j \\ \Delta \phi_j \end{bmatrix} = \sum_{r=1}^{k_j} \mathbf{E}_{j_r}^T \begin{bmatrix} \Delta v_{j_r} \\ \Delta \phi_{j_r} \end{bmatrix} \frac{1}{\sum_{r=1}^{k_j} \frac{1}{z_{j_r,j}}} \tag{A3}$$

where $\mathbf{D}_j = \left[\sin(\omega t + \phi_j),\ v_j \cos(\omega t + \phi_j)\right]^T$ and $\mathbf{E}_{j_r}^T = \left[\frac{\sin(\omega t+\phi_{j_r})}{z_{j_r,j}},\ \frac{v_{j_r} \cos(\omega t+\phi_{j_r})}{z_{j_r,j}}\right]^T$. From small signal stability, we know that the voltage angle change is very small owing to high inertia in rotating parts. Therefore, from (A3) we get

$$\Delta v_j = \sum_{r=1}^{k_j} \sin(\omega t + \phi_{j_r}) z_{j_r,j}^{-1} \Delta v_{j_r} \left(\sin(\omega t + \phi_j) \sum_{r=1}^{k_j} z_{j_r,j}^{-1} \right)^{-1}.$$

Let the instability grid node voltage change be Δv_0, such that $\Delta v_{j_r} = \alpha_{j_r} \Delta v_0$, where α_{j_r} is a constant of multiplication. Substituting this in the previous equation, we get

$$\omega_j = \frac{\Delta v_0}{\Delta v_j} = \frac{\sin(\omega t + \phi_j) \sum_{r=1}^{k_j} z_{j_r,j}^{-1}}{\sum_{r=1}^{k_j} \sin(\omega t + \phi_{j_r}) z_{j_r,j}^{-1} \alpha_{j_r}}. \tag{A4}$$

B. Proof of Lemma 2

It is notable that $z_i^\beta \leq z_i\ \forall\ z_i \in [0,1]$, so $\phi(\mathbf{z}) \leq \sum_{i \in \mathscr{N}} z_k = S\ \forall \mathbf{z} \in \text{Poly}(\mathscr{D}_R)$. Therefore, constraint $\mathbf{C}_1$ forces $\phi(\mathbf{z}) = R$, which is possible iff $z_i^\beta = z_i$, $i \in \mathscr{N}$, i.e., $z_k \in \{0,1\}$, $i \in \mathscr{N}$, implying $\mathbf{z} \in \mathscr{D}_R$.

REFERENCES

[1] A. K. Mandal, A. Malkhandi, S. De, N. Senroy, and S. Mishra, "A multipath model for disturbance propagation in electrical power networks," *IEEE Trans. Circuits Syst. II: Express Briefs*, pp. 1–1, 2022.

[2] L. Huang, J. Coulson, J. Lygeros, and F. Dörfler, "Decentralized data-enabled predictive control for power system oscillation damping," *IEEE Trans. Control Syst. Technol.*, vol. 30, no. 3, pp. 1065–1077, 2021.

[3] R. Gupta, V. Gupta, A. K. Mandal, and S. De, "Learning-based multivariate real-time data pruning for smart PMU communication," in *Proc. IEEE Consumer Commun. Netw. Conf. (CCNC)*, 2022, pp. 326–331.

[4] A. K. Mandal and S. De, "Analysis of wireless communication over electromagnetic impulse noise channel," *IEEE Trans. Wireless Commun.*, pp. 1–1, 2022.

[5] S. Almasabi and J. Mitra, "Multistage optimal PMU placement considering substation infrastructure," *IEEE Trans. Ind. App.*, vol. 54, no. 6, pp. 6519–6528, 2018.

[6] C. D. Patel, T. K. Tailor, S. K. Shukla, S. Shah, and S. N. Jani, "Steiner tree-based design of communication infrastructure with co-optimizing the PMU placement for economical design of WAMS," *IEEE Trans. Instrum. Meas.*, vol. 71, pp. 1–11, 2022.

[7] T. K. Maji and P. Acharjee, "Multiple solutions of optimal PMU placement using exponential binary PSO algorithm for smart grid applications," *IEEE Trans. Indus. Appl.*, vol. 53, no. 3, pp. 2550–2559, 2017.

[8] X.-C. Guo, C.-S. Liao, and C.-C. Chu, "Probabilistic optimal PMU placements under limited observability propagations," *IEEE Syst. J.*, vol. 16, no. 1, pp. 767–776, 2021.

[9] M. K. Arpanahi, H. H. Alhelou, and P. Siano, "A novel multiobjective OPP for power system small signal stability assessment considering WAMS uncertainties," *IEEE Trans. Ind. Informat.*, vol. 16, no. 5, pp. 3039–3050, 2019.

[10] M. Zhang, Z. Wu, J. Yan, R. Lu, and X. Guan, "Attack-resilient optimal PMU placement via reinforcement learning guided tree search in smart grids," *IEEE Trans. Informat. Foren. Secur.*, vol. 17, pp. 1919–1929, 2022.

[11] A. N. Samudrala, M. H. Amini, S. Kar, and R. S. Blum, "Sensor placement for outage identifiability in power distribution networks," *IEEE Trans. Smart Grid*, vol. 11, no. 3, pp. 1996–2013, 2019.

[12] M. Ghamsari-Yazdel, M. Esmaili, F. Aminifar, P. Gupta, A. Pal, and H. Shayanfar, "Incorporation of controlled islanding scenarios and complex substations in optimal WAMS design," *IEEE Trans. Power Syst.*, vol. 34, no. 5, pp. 3408–3416, 2019.

[13] S. Almasabi and J. Mitra, "A fault-tolerance based approach to optimal PMU placement," *IEEE Trans. Smart Grid*, vol. 10, no. 6, pp. 6070–6079, 2019.

[14] Z. M. Ali, S.-E. Razavi, M. S. Javadi, F. H. Gandoman, and S. H. Abdel Aleem, "Dual enhancement of power system monitoring: Improved probabilistic multi-stage PMU placement with an increased search space & mathematical linear expansion to consider zero-injection bus," *Energies*, vol. 11, no. 6, p. 1429, 2018.

[15] A. N. Samudrala, M. H. Amini, S. Kar, and R. S. Blum, "Distributed outage detection in power distribution networks," *IEEE Trans. Smart Grid*, vol. 11, no. 6, pp. 5124–5137, 2020.

[16] M. Shafiullah, M. I. Hossain, M. Abido, T. Abdel-Fattah, and A. Mantawy, "A modified optimal PMU placement problem formulation considering channel limits under various contingencies," *Measurement*, vol. 135, pp. 875–885, 2019.

[17] N. M. Manousakis and G. N. Korres, "Optimal PMU arrangement considering limited channel capacity and transformer tap settings," *IET Gener. Transm. Distrib.*, vol. 14, no. 24, pp. 5984–5991, 2020.

[18] M. H. R. Koochi, P. Dehghanian, and S. Esmaeili, "PMU placement with channel limitation for faulty line detection in transmission systems," *IEEE Trans. Power Deliv.*, vol. 35, no. 2, pp. 819–827, 2019.